



UDC 55.09.35 + 55.22.23

<https://doi.org/10.17073/1997-308X-2023-2-14-34>

Research article
Научная статья



Effects of alloying $\text{ZrB}_2(\text{HfB}_2)\text{--SiC}$ with tantalum on the structure and resistance to high-temperature oxidation and ablation: A review

A. A. Didenko, A. N. Astapov[✉], V. S. Terentieva

Moscow Aviation Institute (National Research University)
4 Volokolamskoe Shosse, Moscow 125993, Russia

✉ lexxa1985@inbox.ru

Abstract. This review presents a comprehensive analysis of the impact of tantalum alloying on the structure, heat resistance, and ablation resistance of $\text{ZrB}_2(\text{HfB}_2)\text{--SiC}$ ultra-high-temperature composites. The influence of the primary phase content on the effects on the structural and morphological features of the oxide layers and their protective efficiency is analyzed. It is shown that alloying positively affects the composite's behavior by enhancing the viscosity and thermal stability of the glass phase, decreasing anionic conductivity, partially stabilizing the $\text{ZrO}_2(\text{HfO}_2)$ lattice, and forming temperature-resistant complex oxides, such as $\text{Zr}_{11}\text{Ta}_4\text{O}_{32}$ or $\text{Hf}_6\text{Ta}_2\text{O}_{17}$ on the surface. It has been established that the alloying can have negative effects, including an increase in the liquid phase content, oxide film discontinuity, $\text{ZrO}_2(\text{HfO}_2)$ grain damage due to TaB_2 oxidation, or a significant amount of gas release due to TaC oxidation, as well as the formation of oxygen diffusion channels during the verticalization of $\text{Zr}_{11}\text{Ta}_4\text{O}_{32}$ or $\text{Hf}_6\text{Ta}_2\text{O}_{17}$ platelets. It is essential to note that the oxidation and ablation resistance, as well as the mechanisms driving composite behavior, differ depending on the alloying compounds and test conditions. Overall, this study sheds light on the role of tantalum alloying in enhancing the performance of $\text{ZrB}_2(\text{HfB}_2)\text{--SiC}$ UHTC and highlights the importance of understanding the underlying mechanisms that govern their behavior.

Keywords: ultrahigh-temperature ceramics (UHTC), heat resistance, oxidation, ablation resistance, oxide film, borosilicate glass, tantalum, alloying

Acknowledgements: This study is supported by the Russian Science Foundation grant No. 22-29-01476, <https://rscf.ru/project/22-29-01476/>.

For citation: Didenko A.A., Astapov A.N., Terentieva V.S. Effects of alloying $\text{ZrB}_2(\text{HfB}_2)\text{--SiC}$ with tantalum on the structure and resistance to high-temperature oxidation and ablation: A review. *Powder Metallurgy and Functional Coatings*. 2023;17(2):14–34. <https://doi.org/10.17073/1997-308X-2023-2-14-34>

Влияние легирования танталом на структуру и стойкость к высокотемпературному окислению и абляции композиций в системе $\text{ZrB}_2(\text{HfB}_2)\text{--SiC}$. Обзор

А. А. Диденко, А. Н. Астапов[✉], В. С. Терентьева

Московский авиационный институт (национальный исследовательский университет)
Россия, 125993, г. Москва, Волоколамское шоссе, 4

✉ lexha1985@inbox.ru

Аннотация. Обзор посвящен изучению состояния вопроса в области влияния легирования соединениями тантала на эволюцию структуры, жаростойкость и стойкость к абляции ультравысокотемпературных композиций на основе системы $\text{ZrB}_2(\text{HfB}_2)$ –SiC. Проанализировано влияние содержания первичных фаз на структурно-морфологические особенности образующихся оксидных слоев и эффективность их защитного действия. Показано, что положительный эффект от легирования прежде всего связан с увеличением вязкости и термической устойчивости формирующейся стеклофазы, снижением анионной проводимости, частичной стабилизацией решетки $\text{ZrO}_2(\text{HfO}_2)$ и образованием на поверхности температуроустойчивых комплексных оксидов типа $\text{Zr}_{11}\text{Ta}_4\text{O}_{32}$ или $\text{Hf}_6\text{Ta}_2\text{O}_{17}$. Установлено, что основными причинами отрицательного влияния легирования являются увеличение доли жидкой фазы, снижение сплошности структуры оксидной пленки в результате повреждения зерен $\text{ZrO}_2(\text{HfO}_2)$ при окислении TaB_2 или образования значительного количества газов при окислении TaC, а также появление дополнительных каналов для диффузии кислорода при вертикализации плоских частиц $\text{Zr}_{11}\text{Ta}_4\text{O}_{32}$ или $\text{Hf}_6\text{Ta}_2\text{O}_{17}$. Отмечено, что характеристики стойкости к окислению и абляции, а также механизмы, определяющие поведение композиций, неодинаковы для разных легирующих добавок и условий испытаний.

Ключевые слова: ультравысокотемпературная керамика (УВТК), жаростойкость, окисление, стойкость к абляции, оксидная пленка, боросиликатное стекло, тантал, модифицирование

Благодарности: Исследование выполнено за счет гранта Российского научного фонда № 22-29-01476, <https://rscf.ru/project/22-29-01476/>.

Для цитирования: Диденко А.А., Астапов А.Н., Терентьева В.С. Влияние легирования танталом на структуру и стойкость к высокотемпературному окислению и абляции композиций в системе $\text{ZrB}_2(\text{HfB}_2)$ –SiC. Обзор. *Известия вузов. Порошковая металлургия и функциональные покрытия*. 2023;17(2):14–34. <https://doi.org/10.17073/1997-308X-2023-2-14-34>

Introduction

Ultra-high-temperature ceramics (UHTC) and composites have been intensively studied as materials suitable for operating under extreme conditions [1–6]. Searching for effective compositions that ensure the operability of products made of them is an urgent problem of modern materials science. Zirconium and hafnium UHTCs have excellent thermomechanical properties, high melting points, and good oxidation resistance when alloyed with SiC. They can operate under extreme temperatures ($>2000^\circ\text{C}$) and in monatomic-oxygen-rich environments [4; 5]. The heterogeneous structure with a refractory crystal oxide matrix and viscous borosilicate glass make this materials extremely heat resistant. Many studies have found that such a structure efficiently withstands the exposure to high-speed, high-enthalpy flows so such materials are the mainstream now [7].

However, work on the modification of $\text{ZrB}_2(\text{HfB}_2)$ –SiC UHTCs is ongoing and there are several reasons for this. In the crystal lattice of refractory ZrO_2 or HfO_2 oxides during oxidation under conditions of oxygen's low partial pressure, as well as when modified with lower valence cations (for example, Y^{3+} , La^{3+}), oxygen vacancies are formed, providing rapid anion transfer through the oxide film [8]. Another problem is ZrO_2 and HfO_2 polymorphism: at high temperatures, the oxides

have a tetragonal or cubic lattice, which transforms into a monoclinic lattice upon cooling, leading to volumetric expansion. This phase transformation, combined with the high coefficient of thermal expansion and low thermal conductivity of the oxides can easily lead to cracking and delamination, especially under thermal cycling loads [8].

To solve this problems, the oxide film can be alloyed with higher valence cations, such as Ta^{5+} or Nb^{5+} . It results in an excess of anions in the lattice and increases film adhesion due to phase stabilization. In addition, the immiscibility of Ta_2O_5 or Nb_2O_5 oxides and borosilicate glass causes phase separation in the surface layer [8], which contributes to the higher viscosity and thermal stability of the glass. Alloying with tantalum is preferable, since the partial pressures of vapors over Ta_2O_5 are significantly lower when compared to Nb_2O_5 at high and ultra-high temperatures. Tantalum can be added in the form of a pure element, boride, silicide, or carbide. Some properties of these substances are listed in Table 1.

This review aims to analyze the available studies of tantalum alloying effects on the structure and behavior of materials based on $\text{ZrB}_2(\text{HfB}_2)$ –SiC in the oxidizing atmosphere, as well as to identify the mechanisms of their impact on the oxidation and ablation resistance. We considered various types of materials:

Table 1. Ta composition properties [9–14]

Таблица 1. Свойства Ta-содержащих соединений [9–14]

Property	Ta	TaB ₂	TaB	TaSi ₂	Ta ₅ Si ₃	TaC
Density, g/cm ³	16.40–16.65	11.20–12.62	14.00–14.29	8.80–9.14	12.50–13.06	14.30–14.80
Melting point, °C	2996–3020	3037–3200	2040–3090	2040–2299	2499–2550	3800–3880
Thermal expansion coefficient, 10 ⁻⁶ /K	6.3–6.6	8.2–8.8	–	7.4–8.5	–	6.64–8.4
Specific heat capacity, J/(kg·K)	140.00	237.55	246.85	–	–	190.00
Thermal conductivity, W/(m·K)	57.5	10.9–16.0	–	37.0	–	22.2

bulk UHTC, heat-resistant UHTC coatings on graphite and carbon-carbon composites, and carbon-ceramic composites with a UHTC matrix.

1. Bulk tantalum-alloyed ZrB₂(HfB₂)–SiC ultrahigh-temperature ceramics

In oxidizing environments, the structure of zirconium and hafnium diboride UHTCs alloyed with SiC becomes layered, including a continuous glass layer, a sublayer of the ZrO₂ and HfO₂ refractory oxides containing heat-resistant particles ZrSiO₄ and HfSiO₄, respectively, a layer of ZrB₂ and HfB₂ depleted in SiC, and a layer of unreacted ceramic [15–17]. Temperatures above the silicon dioxide melting point (1723 °C [18]) intensify the evaporation and mechanical removal of the glass by the high-speed flows [19], so the purpose of alloying with tantalum compounds is mostly connected with an increase in the UHTC oxidation and ablation resistance. Most studies do confirm the positive effects of Ta alloying. However, the results are inconsistent and are highly dependent on the test conditions.

1.1. Tantalum borides effects on ZrB₂–SiC structure and oxidation resistance

The Ta–B system has five intermediate phases: TaB₂, Ta₃B₄, TaB, Ta₂B, and Ta₃B. Only TaB and TaB₂ are stable in the room temperature to melting point range [14] and can be used as UHTC alloying components. Talmy I. et al. [20] reported that alloying the ZrB₂–SiC ceramics with tantalum diboride (10 mol. %) significantly increases its oxidation resistance

at 1300 °C. The oxide film on the TaB₂ containing samples was less than a half of that on the reference UHTC samples. It was also found that adding even 2 mol. % TaB₂ results in a significant oxidation resistance growth when the sample is heated in a furnace at $t = 1200\div1400$ °C for 2 h. The morphology of the resulting heterogeneous surface layer indicates the spinodal decomposition of the SiO₂–Ta₂O₅ phases [20]. However, at $t = 1500$ °C no pronounced positive effect of TaB₂ additions on the ZrB₂–SiC heat resistance was observed. This may be associated with exceeding the miscibility limit of the multicomponent SiO₂–Ta₂O₅–ZrO₂ oxide system.

Lee S. et al. [15] studied the effects of adding tantalum to the ZrB₂–SiC system and the oxidation resistance of the (Zr_{0.7}Ta_{0.3})B₂ ceramic composite containing 30 vol. % SiC at temperatures up to 1500 °C and low partial oxygen pressure ($\sim 10^{-8}$ Pa). The weight gain of the Ta-containing samples, mostly attributed to the oxidation of ZrB₂ and TaB₂ to ZrO₂ and Ta₂O₅ occurs starting at 1000 °C, which is above the oxidation start temperature in UHTCs without Ta (800 °C). Lee S. et al. attributed the higher oxidation resistance in the material alloyed with TaB₂ over the entire temperature range primarily to the formation of a less porous oxide sublayer under the SiO₂-containing film. This was explained by the high viscosity of the liquid phase in the SiO₂–Ta₂O₅ system which is less susceptible to upwelling to the amorphous surface layer [15; 21]. Also, they observed a decrease in the (Zr_{0.7}Ta_{0.3})B₂ particle size, higher modulus of elasticity, hardness, and fracture toughness of the UHTC.

Peng F. et al. [22] studied the oxidation resistance of ZrB₂–B₄C–SiC–TaB₂ containing B₄C as a sintering additive [21] in the 1200–1500 °C temperature range. Increasing the TaB₂ concentration from 3.32 to 16.61 mol. % results in slightly better heat resistance at $t = 1200$ and 1400 °C. At $t = 1500$ °C, small

(3.32 mol. %) amounts of TaB_2 also improve the oxidation resistance [22]. Alloying with TaB_2 reduces the thickness of the oxide sublayers, but has no significant effect on the thickness of the amorphous surface layer. The researchers explained the higher heat resistance by the better sealing of oxide sublayers as their microstructure branches, since dispersed TaC particles are formed (it is a thermodynamically possible product of TaB_2 and SiC oxidation) [22] and also due to a larger surface wetted by the liquid phase. This contributes to reduced upwelling of the glass phase into the surface layer [23]. The higher TaB_2 concentration decreases the oxidation resistance at $t = 1500^\circ\text{C}$ (and accelerates the weight gain after 60 and 120 min for 16.61 and 13.29 mol. % TaB_2 concentrations, respectively) [22], due to easier dissolution and deposition of zirconium dioxide in the glass surface layer [20].

The oxidation of $\text{ZrB}_2\text{-B}_4\text{C-SiC-TaB}_2$ containing 3.32 mol. % TaB_2 was also studied in the $1500\text{--}1900^\circ\text{C}$ temperature range [23]. The samples after oxidation feature thinner oxide passivation layers compared to TaB_2 -free samples, and have a high oxidation resistance.

The effect of TaB monoboride on the oxidation of $\text{ZrB}_2\text{-SiC}$ UHTC was also investigated at $t = 1800^\circ\text{C}$ [24]. Ta adding greatly influences oxidation resistance, due to the evolution of the oxide film structure and the oxygen transport pathway during exposure. However, the effect on the UHTC oxidation resistance is significantly different from that at lower temperatures. For instance, ceramics alloyed with TaB show the lowest heat resistance at $t = 1800^\circ\text{C}$ among CrB_2 , HfB_2 and TaB alloying compounds [24].

1.2. Structure and oxidation resistance of $\text{ZrB}_2(\text{HfB}_2)\text{-SiC}$ with tantalum carbides additions

Tantalum carbide has one of the highest melting points and can also be used as an additive [25], thus increasing the oxidation resistance of $\text{ZrB}_2\text{-SiC}$ and $\text{HfB}_2\text{-SiC}$ ceramic materials. However, Opila E. et al. [26] discovered that adding 20 vol. % TaC to $\text{ZrB}_2\text{-SiC}$ does not increase the heat resistance. The TaC-containing samples at $t = 1627^\circ\text{C}$ form a non-gastight film, presumably

due to the porous microstructure formed by the CO and/or CO_2 release during oxidation.

The oxidation patterns of $\text{ZrB}_2\text{-SiC-TaC}$ samples with different TaC contents (10 and 30 vol. %) in the $t = 1200\text{--}1500^\circ\text{C}$ temperature range indicate [27] that low TaC concentrations accelerate the oxidation, when compared to $\text{ZrB}_2\text{-SiC}$ (the oxidation rate at $t = 1500^\circ\text{C}$ increases 8-fold). Still, high TaC concentrations significantly improve the resistance to oxidation in air. For example, a sample containing 30 vol. % TaC showed an oxidation rate half as high as that of the initial ceramics under the same conditions. The surface of oxidized UHTCs containing TaC features multilayer oxide films including [27]:

- 1) a thin top layer of silicon dioxide;
- 2) a layer containing a mixture of the $\text{ZrO}_2\text{-SiO}_2\text{-Ta}_2\text{O}_5$ (10 vol. % TaC) and $\text{ZrO}_2\text{-SiO}_2\text{-ZrSiO}_4$ (30 vol. % TaC) phases;
- 3) a layer with a high Ta_2O_5 content.

It should be noted that these layers are porous in UHTCs with low TaC concentrations (in contrast to the samples with high TaC concentrations, where all the three oxide layers are very dense), and the oxide film thickness after oxidation at $t = 1500^\circ\text{C}$ for 10 h is $850\text{ }\mu\text{m}$ (vs. $140\text{ }\mu\text{m}$ for $\text{ZrB}_2\text{-SiC-30 vol. \% TaC}$ and $440\text{ }\mu\text{m}$ for $\text{ZrB}_2\text{-SiC}$).

Re-oxidation of the same samples at $t = 1500^\circ\text{C}$ showed that the oxidation may be caused not only by the inward diffusion of oxygen. For instance, cations diffusing from ceramics into the oxides, according to Wang Y. et al. [27] are also initially involved in mass transfer. The oxidation of $\text{ZrB}_2\text{-SiC-10 vol. \% TaC}$ is governed by the outward diffusion of tantalum resulting in the rapid formation of a porous structure, while the oxidation of $\text{ZrB}_2\text{-SiC-30 vol. \% TaC}$ is governed by the outward diffusion of silicon resulting in the formation of a dense SiO_2 layer and a significant share of the ZrSiO_4 heat-resistant phase.

The $\text{ZrB}_2\text{-20 vol. \% SiC}$ material with 5 vol. % TaC [28] also has a multilayer structure after oxidation at $t = 1400^\circ\text{C}$. The four layers that reacted with oxygen were observed:

- 1) a thin top layer of silicon dioxide containing Ta_2O_5 ;
- 2) a layer containing the ZrO_2 , ZrSiO_4 and SiO_2 phases;

- 3) a layer enriched in ZrO_2 and depleted in SiC ;
- 4) a ZrB_2 -depleted layer containing SiO_2 and Ta_2O_5 .

The oxide film on a similar material oxidized at $t = 1700^\circ C$ contains the ZrO_2 , Ta_2O_5 , SiO_2 and $ZrSiO_4$ phases [28]. It follows that all the UHTC components including the initial ZrB_2 , SiC and TaC , as well as the *in situ* formed ZrC and $TaSi_2$ phases, are oxidized under a high-temperature exposure.

Simonenko E. et al. [29] proposed adding the Ta_4HfC_5 complex carbide to HfB_2-SiC (5, 10, 15 vol. %), in order to prevent the HfB_2 grain growth, which improves the mechanical properties of the ceramics (note Ta_4HfC_5 is a nanodisperse phase). The thermogravimetric analysis of the ceramics samples when heated in air flow to $1400^\circ C$ showed that the increase of Ta_4HfC_5 content leads to the increase of the sample weight gain due to oxidation. The materials are more sensitive to oxygen than HfB_2-SiC , that can be explained by the high reactivity of the Ta_4HfC_5 ultra-heat-resistant nanocrystalline carbides and significant porosity. The microstructure of the oxidized sample surface depends on the Ta_4HfC_5 content. The UHTC containing 15 vol. % of the complex carbide is most noticeable: the silicon monoxide fibers on the borosilicate glass surface are self-organized into regular, hierarchical 3D nanostructures.

Simonenko E. et al. [30] exposed HfB_2-30 vol. % $SiC-10$ vol. % Ta_4HfC_5 to a high-enthalpy air jet for 2000 s under conditions of a gradual increase in the plasm generator anode power from 30 to 70 kW, and the heat flux from 363 to 779 W/cm². A distinctive feature of the ceramics under heating is a decrease of the surface radiative equilibrium temperature relative to the HfB_2-30 vol. % SiC reference material under identical test conditions. As the authors proposed, it is associated with the higher thermal conductivity of the ceramics alloyed with the Ta_4HfC_5 nanodisperse carbide. The tantalum oxide formed by Ta_4HfC_5 oxidation is a part of the silicate glass [30] and involved in the creation of the $Hf_6Ta_2O_{17}$ orthorhombic complex oxide which has phase stability up to the peritectic transformation point at $t \sim 2250^\circ C$ [31]. The lower evaporation rate from the glassy layer surface is attributed to the lower surface temperature and lower vapor pressure over the $SiO_2-Ta_2O_5$ melt (the total vapor pressure at $t = 1827^\circ C$ over SiO_2 (mostly SiO) and Ta_2O_5 (TaO_2 and TaO) is $9.48 \cdot 10^{-5}$ and $7 \cdot 10^{-7}$ atm, respectively [30]). As the surface temperature reached $1750 \div 1850^\circ C$, even for the max heat flux, no “tem-

perature jump” characteristic $HfB_2(ZrB_2)-SiC$ [32] was observed.

1.3. Effects of tantalum silicides on $ZrB_2(HfB_2)-SiC$ structure and oxidation resistance

Tantalum silicides are highly refractory (the melting point exceeds $2000^\circ C$ [9; 11]), can be used as sintering additives [33–35] and an additional source of silicon [36; 37], in order to facilitate the formation of protective silicate glass layers of the UHTC surface. Peng F. et al. [21] reported that adding 6.6 mol. % $TaSi_2$ to ZrB_2-B_4C-SiC resulted in higher oxidation resistance in the $1200 \div 1400^\circ C$ temperature range compared with TaB_2 . The reason is that the formation of a protective surface glass layer with phase separation is facilitated by both Ta and extra Si, the oxidation of which increases the amount of the liquid phase and changes its composition. However, at $t = 1500^\circ C$ the tantalum disilicide produces an opposite effect: $TaSi$ concentration increase above 3.32 mol. % results in lower heat resistance, although the decrease is not as significant as the one caused by the TaB_2 content increase. Nevertheless, at low concentrations (3.3 mol. %) TaB_2 is more efficient compared to $TaSi_2$ at $t = 1500^\circ C$ [22], and the lowest weight gain was observed in a mixture of TaB_2 and $TaSi_2$ (3.4 and 3.3 mol. %, respectively) over the entire temperature range [21].

The addition of $TaSi_2$ significantly improved the relative density, thermal shock resistance, and antioxidant properties of ZrB_2-SiC at $t = 1000 \div 1600^\circ C$ [38]. The specific gravity variation over the entire thermal shock temperature range for the $TaSi_2$ -containing samples was significantly less than that of the original samples: at $t = 1600^\circ C$ the weight of ZrB_2-5 wt. % $SiC-15$ wt. % $TaSi_2$ changed by 0.68 %, whereas the weight of ZrB_2-5 wt. % SiC , by 1.6 %. The weight variation decreases as the $TaSi_2$ content increases [38].

Opila E. et al. [39] discovered that adding 5 vol. % $TaSi_2$ to ZrB_2-20 vol. % SiC was not sufficient to induce phase separation in the glass and improve the oxidation resistance in stagnant air at $t = 1627^\circ C$. On the other hand, the composition containing 20 vol. % $TaSi_2$ has better oxidation resistance compared to the original material. The oxide film thickness on the ZrB_2-20 vol. % $SiC-20$ vol. % $TaSi_2$ sample decreased about 10-fold when compared to the reference ceramics, and the surface appearance indicated the immiscibility

of the glass phases [8; 26]. Under more extreme conditions (holding for 50 min in stagnant air at $t = 1927^\circ\text{C}$), the ceramics containing 20 vol. % TaSi_2 showed lower heat resistance compared to the non-alloyed material, as a result of forming a significant amount of the liquid phase [26]. Attempts to reduce its amount by reducing the TaSi_2 content to 5 vol. % were unsuccessful. The amount of liquid phase dropped compared to ZrB_2 –20 vol. % SiC–20 vol. % TaSi_2 , but its share was still substantial [39]. The TaSi_2 applications at $t = 1927^\circ\text{C}$ are limited for several reasons:

1) TaSi_2 is unstable in the matrix with respect to ZrB_2 ;

2) TaSi_2 oxidizes intensively in the presence of SiC producing TaC and gaseous SiO which makes gaps in the substrate;

3) During the oxidation, 1.3 at. % or less of tantalum dissolves in ZrO_2 , i.e. *in situ* alloying of zirconium dioxide to reduce the rate of oxygen transfer through it is limited;

4) The oxidation forms oxiboride, silicate, and zirconate phases, which leads to the formation of a large amount of liquid phase, and poor oxidation resistance.

Julian-Jankowiak A. et al. [40] also observed an increase of the ZrB_2 –20 vol. % SiC–20 vol. % TaSi_2 oxidation resistance to 1900°C and its decrease at higher temperatures (the heat resistance was studied at $t = 1200\div 2300^\circ\text{C}$ in air and water vapor).

With regard to hafnium diboride-based ceramics, the oxidation resistance of HfB_2 –20 vol. % SiC in air at $t = 1627^\circ\text{C}$ deteriorated after adding 20 vol. % TaSi_2 [26]. Monteverde F. et al. [35] obtained similar results for HfB_2 –30 vol. % SiC–2 vol. % TaSi_2 produced by hot pressing (HP) and spark plasma sintering (SPS): the material heat resistance in air deteriorated in the $t = 1450\div 1650^\circ\text{C}$ range compared to TaSi_2 -free materials. The microstructure of the oxidized samples was characterized by the presence of a layered oxide film, which thickness increased with temperature [35].

1.4. Metallic tantalum use to control ZrB_2 –SiC structure and oxidation resistance

Tantalum in the form of a metal additive is also of interest, since it can be used to reduce sintering temperature, increase density, and improve the machi-

nability, mechanical, and thermal properties of ZrB_2 –SiC [41–43]. Thimmappa S. et al. [44; 45] showed that ZrB_2 –20 vol. % SiC (2.5–10.0) wt. % Ta contains ZrB_2 cores in $(\text{Zr}, \text{Ta})\text{B}_2$ shells, and also contains SiC, ZrO_2 and $(\text{Zr}, \text{Ta})\text{C}$ phases at the interfaces between the ZrB_2 grains. It was shown that tantalum dissolves in the ZrB_2 matrix, thus building a shell from the solid solution phase [41]. Hu C. et al. [33], Silvestroni L. et al. [37] and Yang Y. et al. [46] observed similar structures. The alloying with tantalum has a positive effect on the heat resistance of ZrB_2 –20 vol. % SiC samples [44]. As the Ta content increases, the specific gravity and thickness of the oxide layer after isothermal oxidation at $t = 1500^\circ\text{C}$ for 10 h in the air decreases from 22.91 to 18.77 mg/cm² and from 401 to 195 μm , respectively. Thimmappa S. et al. [45] observed a similar trend at $t = 1600^\circ\text{C}$ (refer to Table 2).

The cross-section microstructure of the ZrB_2 –SiC–Ta samples oxidized at $t = 1500$ and 1600°C consists of three layers:

- 1) a thick, dense outer SiO_2 layer;
- 2) an intermediate ZrO_2 sublayer;
- 3) a ZrB_2 layer, depleted in SiC.

After oxidation, the material contains the ZrO_2 , $\text{Zr}_{2.75}\text{TaO}_8$ crystalline phases, and the SiO_2 amorphous silica [44; 45]. The $\text{Zr}_{2.75}\text{TaO}_8$ phase formation is thermodynamically feasible at $t = 1500^\circ\text{C}$, and the phase content increases with the Ta concentration resulting in a higher viscosity of the glass phase and higher oxidation resistance [45]. As the Ta content increases, the thickness of the SiC-depleted layer decreases, and this can be attributed to the effects of the SiO_2 -based, tantalum-modified top passivation layer [45].

It is assumed that the SiC-depleted layer reduces the overall oxidation resistance of ZrB_2 ceramic materials. However, no defects were found on the surface of ZrB_2 –20 vol. % SiC–10 wt. % Ta with a SiC-depleted layer formed by isothermal oxidation at $t = 1600^\circ\text{C}$ for 10 h in air. The UHTC showed comparable weight gain, and a significantly lower oxygen penetration depth (255 vs. 476 μm) than ZrB_2 –20 vol. % SiC–10 vol. % Si_3N_4 without such a layer [41]. In general, ZrB_2 –SiC–Ta ceramics have favorable strength at elevated temperatures [45] and heat resistance due to the protective nature of the formed oxide film. These UHTCs are suitable for high-temperature applications [41].

Table 2. Oxidation resistance of $\text{ZrB}_2(\text{HfB}_2)\text{--SiC}$ alloyed with Ta and Ta compounds

 Таблица 2. Характеристики окислительной стойкости керамик на основе $\text{ZrB}_2(\text{HfB}_2)\text{--SiC}$, модифицированных танталом и его соединениями

Composition, vol. %	Manufacturing process	Oxidation properties			Phase composition after oxidation	Reaction layer thickness, μm	Weight change, mg/cm^2	Reference
		t , $^\circ\text{C}$	Time, min	Test conditions				
$\text{ZrB}_2\text{--}20\text{SiC} + 2.5 \text{ wt. \% Ta}$	SPS (1900 $^\circ\text{C}$, 50 MPa, 3 min)	1500	600	Furnace, stagnant air	SiO_2 , ZrO_2 , $\text{Zr}_{2.75}\text{TaO}_8$	401	22.91	[44]
		1600				320	21.04	[45]
$\text{ZrB}_2\text{--}5.6\text{B}_4\text{C--}27.9\text{SiC} + 3.3 \text{ mol. \% TaSi}_2$	Sintering (2000 $^\circ\text{C}$, Ar, 1 h)	1500	240	TGA, air (0.1 l/min)	$m,o\text{--ZrO}_2$, TaC	~9	~7.9	[22]
$\text{ZrB}_2\text{--}5.6\text{B}_4\text{C--}27.9\text{SiC} + 3.3 \text{ mol. \% TaB}_2$	HIP (1800 $^\circ\text{C}$, 207 MPa, 30 min)					~24	~5.7	
$\text{ZrB}_2\text{--}5.6\text{B}_4\text{C--}27.9\text{SiC} + 3.3 \text{ mol. \% TaB}_2$	Sintering (2100 $^\circ\text{C}$, Ar, 1 h) HIP (1800 $^\circ\text{C}$, 207 MPa, 30 min)	1600	75	TGA, air (0.1 l/min)	$\text{Zr}_x\text{Ta}_{1-x}\text{B}_2$, ZrC(traces)	~166	~5.9	[23]
		1700	90			~395	~6.8	
		1800	85			~416	~11	
		1900	85			–	~15	
$\text{ZrB}_2\text{--}25\text{SiC} + 5 \text{ mol. \% TaB}_2$	HP (2100 $^\circ\text{C}$, 20 MPa, 30 min)	1400	120	Furnace, stagnant air	–	–	~4.6	[20]
$\text{ZrB}_2\text{--}20\text{SiC--}5\text{TaC}$	HP (1850 $^\circ\text{C}$, 40 MPa, 60 min)	1400	600	Furnace, stagnant air	SiO_2 , Ta_2O_5 , ZrO_2 , ZrSiO_4	~65	–	[28]
$\text{ZrB}_2\text{--}20\text{SiC} + 5 \text{ wt. \% Ta}$	SPS (1900 $^\circ\text{C}$, 50 MPa, 3 min)	1500	600	Furnace, stagnant air	SiO_2 , ZrO_2 , $\text{Zr}_{2.75}\text{TaO}_8$	384	19.15	[44]
		1600				303	17.45	[45]
$\text{ZrB}_2\text{--}20\text{SiC--}5\text{TaSi}_2$	HP (1750 $^\circ\text{C}$, 69 MPa, 2 h)	1627	100	Bottom-loading furnace, stagnant air	$m,c\text{--ZrO}_2$	–	~5.1	[39]
$\text{ZrB}_2\text{--}5.6\text{B}_4\text{C--}27.9\text{SiC} + 6.6 \text{ mol. \% TaB}_2$	Sintering (2000 $^\circ\text{C}$, Ar, 1 h)	1460	–	TGA, air (0.1 l/min)	$\text{ZrB}_2\text{--TaB}_2(\text{ss})$, ZrO_2 , TaC, TaO (следы)	~25	~2.6	[21]
$\text{ZrB}_2\text{--}5.6\text{B}_4\text{C--}28\text{SiC} + 6.7 \text{ mol. \% TaSi}_2$	HIP (1800 $^\circ\text{C}$, 207 MPa, 30 min)					–	~1.0	
$\text{ZrB}_2\text{--}5.6\text{B}_4\text{C--}27.9\text{SiC} + 6.7 \text{ mol. \% TaB}_2$	Sintering (2000 $^\circ\text{C}$, Ar, 1 h) HIP (1800 $^\circ\text{C}$, 207 MPa, 30 min)	1500	240	TGA, air (0.1 l/min)	$m,o\text{--ZrO}_2$, TaC	~42	~13.2	[22]
$\text{ZrB}_2\text{--}5.6\text{B}_4\text{C--}27.9\text{SiC} + 6.7 \text{ mol. \% TaSi}_2$					$m,o\text{--ZrO}_2$, TaC, $\text{ZrB}_2\text{--TaB}_2(\text{ss})$	~10.7	~8.1	
$\text{ZrB}_2\text{--}5.6\text{B}_4\text{C--}27.9\text{SiC} + 10 \text{ mol. \% TaB}_2$					$m,o\text{--ZrO}_2$, TaC	~45	~17.5	
$\text{ZrB}_2\text{--}5.6\text{B}_4\text{C--}27.9\text{SiC} + 10 \text{ mol. \% TaSi}_2$					$m,o\text{--ZrO}_2$, TaC, $\text{ZrB}_2\text{--TaB}_2(\text{ss})$	~13	~10	

Table 2. Oxidation resistance of $\text{ZrB}_2(\text{HfB}_2)\text{--SiC}$ alloyed with Ta and Ta compounds (Continuation)Таблица 2. Характеристики окислительной стойкости керамик на основе $\text{ZrB}_2(\text{HfB}_2)\text{--SiC}$, модифицированных танталом и его соединениями (продолжение)

Composition, vol. %	Manufacturing process	Oxidation properties			Phase composition after oxidation	Reaction layer thickness, μm	Weight change, mg/cm ²	Refe- rence
		<i>t</i> , °C	Time, min	Test conditions				
ZrB ₂ –25SiC + 10 mol. % TaB ₂	HP (2100 °C, 20 MPa, 30 min)	1400	300	TGA, Ar/O ₂ mixture (125 cm ³ /min)	ZrO ₂ , Zr _{2.75} TaO ₈	~50	–	[20]
ZrB ₂ –20SiC + 10 wt. % Ta	SPS (1900 °C, 50 MPa, 3 min)	1500	600	Furnace, stagnant air	SiO ₂ , ZrO ₂ , Zr _{2.75} TaO ₈	195	18.77	[44]
ZrB ₂ –20SiC– 10TaC	HP (1800 °C, 28 MPa, 1 h)	1500	600	Furnace, heating/ cooling: Ar, oxidation: air (10 ml/min)	ZrO ₂ , Ta ₂ O ₅	850	~58	[27]
ZrB ₂ –20SiC + 10 wt. % Ta	SPS (1900 °C, 50 MPa, 3 min)	1600	600	Furnace, stagnant air	SiO ₂ , ZrO ₂ , Zr _{2.75} TaO ₈	255	16.65	[41; 45]
ZrB ₂ –20SiC– 10TaB	HP (2000 °C, 30 MPa, 1 h)	1800	60	Bottom- loading furnace, stagnant air	–	–	~68	[24]
ZrB ₂ –5.6B ₄ C– 27.9SiC + 13.3 mol. % TaB ₂	Sintering (2000 °C, Ar, 1 h) HIP (1800 °C, 207 MPa, 30 min)	1460	–	TGA, air (0.1 l/min)	ZrB ₂ – TaB ₂ (ss), ZrO ₂ , TaC	–	~0.9	[21]
ZrB ₂ –5.6B ₄ C– 27.9SiC + 13.3 mol. % TaB ₂		1500	240		<i>m,o</i> -ZrO ₂ , TaC, TaB ₂	~67	~23.1	[22]
ZrB ₂ –5.6B ₄ C– 27.9SiC + 13.3 mol. % TaSi ₂						~12.5	~11.6	
ZrB ₂ –5SiC + 15 wt. % TaSi ₂	SPS (1700 °C, 50 MPa, 10 min)	1600	–	Thermal shock test	ZrB ₂ , ZrO ₂ , Zr–Ta–B, Zr–Ta–O	–	0.68%	[38]
ZrB ₂ –20SiC– 20TaC	HP (2000 °C, 69 MPa, 2 h)	1627	100	Bottom- loading furnace, stagnant air	<i>t,m</i> -ZrO ₂	–	~21	[26]
ZrB ₂ –20SiC– 20TaSi ₂	HP (1600 °C, 69 MPa, 2 h)	1627	100	Bottom- loading furnace, stagnant air	<i>m,c</i> -ZrO ₂ , SiO ₂	–	~0,8	[8; 26]
(Zr _{0.7} Ta _{0.3})B ₂ – 30SiC	HP (1800 °C, Ar, 32 MPa, 2 h)	1500	60	Furnace, CO and 2000 ppm CO ₂ mixture (~10 ^{–8} Pa)	–	10.1±1.2	–	[15]
			600		–	72.3±2.8	–	
			300		TGA, air	–	–	
ZrB ₂ –20SiC– 30TaC	HP (1800 °C, 28 MPa, 1 h)	1500	600	Furnace, heating/ cooling: Ar, oxidation: air (10 ml/min)	ZrSiO ₄ , Ta ₂ O ₅ , ZrO ₂ , SiO ₂	140	~13	[27]

Table 2. Oxidation resistance of $\text{ZrB}_2(\text{HfB}_2)\text{--SiC}$ alloyed with Ta and Ta compounds (Completion)

 Таблица 2. Характеристики окислительной стойкости керамик на основе $\text{ZrB}_2(\text{HfB}_2)\text{--SiC}$, модифицированных танталом и его соединениями (окончание)

Composition, vol. %	Manufacturing process	Oxidation properties			Phase composition after oxidation	Reaction layer thickness, μm	Weight change, mg/cm^2	Reference
		t , $^\circ\text{C}$	Time, min	Test conditions				
$\text{HfB}_2\text{--}30\text{SiC--}2\text{TaSi}_2$	HP (1900 $^\circ\text{C}$, 42 MPa, 35 min)	1450	1200	TGA, dry air (15 cm^3/min)	–	–	4.1	[35]
		1500	60	Furnace, stagnant air	–	–	0.79	
		1650			–	–	6.27	
	SPS (2100 $^\circ\text{C}$, 30 MPa, 3 min)	1450	1200	TGA, dry air (15 cm^3/min)	–	–	3.3	
		1500	60	Furnace, stagnant air	–	–	0.94	
		1650			–	–	2.85	
$(\text{HfB}_2\text{--}30\text{SiC})\text{--}5\text{Ta}_4\text{HfC}_5$	HP + reaction (1800 $^\circ\text{C}$, Ar, 30 MPa, 30 min)	1400	–	DSC/TGA, air (250 ml/min)	$m\text{--HfO}_2$, HfB_2	–	2.10 %	[29]
$(\text{HfB}_2\text{--}30\text{SiC})\text{--}10\text{Ta}_4\text{HfC}_5$		1400	–			–	2.96 %	
$(\text{HfB}_2\text{--}30\text{SiC})\text{--}10\text{Ta}_4\text{HfC}_5$		779 W/ cm^2	33.3	Plasma generator, air (3.6 g/s)	$m,o\text{--Ta}_2\text{O}_5$, $o\text{--Hf}_6\text{Ta}_2\text{O}_{17}$	–	5.9 %	[30]
$(\text{HfB}_2\text{--}30\text{SiC})\text{--}15\text{Ta}_4\text{HfC}_5$		1400	–	DSC/TGA, air (250 ml/min)	$m\text{--HfO}_2$, HfB_2 , Ta_2O_5	–	3.27 %	[29]
$\text{HfB}_2\text{--}20\text{SiC--}20\text{TaSi}_2$	HP (1700 $^\circ\text{C}$, 69 MPa, 2 h)	1627	100	Bottom-loading furnace, stagnant air	$m,c\text{--HfO}_2$, HfSiO_4	–	~2.5	[26]

Abbreviations: (ss) – solid solution; HIP – hot isostatic pressing; TGA – thermogravimetric analysis; DSC – differential scanning calorimetry.

2. Heat-resistant coatings on graphite and C/C composites based on $\text{ZrB}_2(\text{HfB}_2)\text{--SiC}$ alloyed with tantalum compounds

An alternative approach is applying UHTC coatings to heat-resistant, carbon-containing composites, and graphite [47–50]. In order to protect carbon-containing materials from oxidation, ceramic coatings should have the following properties [11; 51; 52]:

- 1) heat resistance in a wide temperature range;
- 2) high adhesion, and compatibility with the substrate;

3) coating continuity and oxide film gas tightness for erosion resistance and limiting oxygen diffusion to the substrate;

4) self-healing of the coating defects;

5) high manufacturability, process consistency, controlled coating thickness, and coating reparability.

Multilayer ceramic coatings with transition metal diborides and silicon carbide are effective for increasing the oxidation resistance of carbon-containing composites by preventing oxygen penetration to the substrate. They form a silicate glass layer on the surface, and a sublayer based on refractory oxides [53; 54]. However, the protective properties of such coatings are very limited: 265 and 550 h for C/C composi-

tes with HfB_2 –SiC/SiC and ZrB_2 –SiC/SiC coatings at $t = 1500^\circ\text{C}$, respectively.

In real-life applications, the coatings should maintain the long-term performance of the carbon material in oxidizing environments in a wide temperature range, under static and dynamic loads. Therefore, an extremely important is the creation of ultra-high-temperature, durable protective coatings highly resistant to oxidation and erosion. It was proposed that tantalum be added to $\text{ZrB}_2(\text{HfB}_2)$ –SiC compositions, in order to obtain multiphase coatings with good heat and ablation resistance due to the synergistic effect of the two cationic compounds exposed to a high-temperature, oxygen-containing environment [54].

2.1. Tantalum boride-alloyed $\text{ZrB}_2(\text{HfB}_2)$ –SiC coatings

The addition of UHTC borides to SiC-based coatings expands the operating temperature range and improves antioxidation properties by increasing the glassy surface layer viscosity and reducing crack formation. Furthermore, B_2O_3 formed during oxidation can heal coating defects and improve resistance to low-temperature oxidation [55–57]. To protect graphite from oxidation, Jiang Y. et al. [56] applied a single-layer, multi-phase $(\text{Zr}, \text{Ta})\text{B}_2$ –SiC–Si coating, demonstrating oxidation resistance for 468 h at 1000°C and for 347 h at 1500°C . The coating structure after oxidation includes two layers: external Zr–Ta–Si–O (glass), and internal $(\text{Zr}, \text{Ta})\text{B}_2$ –SiC–Si. The continuous oxide film on the surface has low oxygen permeability and effectively reduces the coating oxidation rate [56].

The $\text{Ta}_{0.5}\text{Zr}_{0.5}\text{B}_2$ –Si–SiC dense, single-layer multiphase ceramic coating protects graphite from oxidation at 1650°C for at least 70 h due to the synergistic effect of the heterogeneous oxide layer formed during oxidation and the dense inner coating [55]. Also, the $\text{Ta}_{0.5}\text{Zr}_{0.5}\text{B}_2$ –Si–SiC coating is resistant to ablation when exposed to heat fluxes ($2.4\div 4.2\text{ MW/m}^2$). It was found that increasing the heat flux of the oxyacetylene flame resulted in more intense weight loss and thinning of the coating, and its ablation behavior varied from oxidation and evaporation at 2.4 MW/m^2 to mechanical removal at 4.2 MW/m^2 [55]. Note that after ablation for 40 s under a 4.2 MW/m^2 heat flux, a new microstructure consisting of “lath-like” grains ($\text{Ta}_4\text{Zr}_{11}\text{O}_{32}$ solid solution) with few micropores and high erosion

resistance was found at the heat flux center. The surface oxide layer contains $\text{Ta}_4\text{Zr}_{11}\text{O}_{32}$, ZrO_2 and Ta_2O_5 . These phases provide efficient protection of the material below from ablation. The inner $\text{Ta}_{0.5}\text{Zr}_{0.5}\text{B}_2$ –Si–SiC coating protected by the outer oxide layer mostly faces high-temperature oxidation and the release of gaseous SiO and CO.

Jiang Y. et al. [57] manufactured a defect-free, single-layer multi-phase $\text{Hf}_{0.5}\text{Ta}_{0.5}\text{B}_2$ –SiC–Si coating on graphite. After oxidation in air at $t = 1500^\circ\text{C}$, the coating surface contained $\text{Ta}_{0.5}\text{B}_2$, Ta_2O_5 , SiO_2 and HfSiO_4 (hafnon is the product of the reaction between HfO_2 and SiO_2 [58]), i.e., a complex silicate oxide layer, emerges to prevent oxygen from entering into the coating. The coating is resistant to low- and high-temperature isothermal oxidation for 1320 h at $t = 900^\circ\text{C}$ and for 2080 h at $t = 1500^\circ\text{C}$ (the weight gains were 0.14 % and 1.74 %, respectively), and also has good ablation resistance [57]. Jiang Y. et al. [57] explained the high resistance to oxidation at $t = 900^\circ\text{C}$ by the defect-free coating structure, and at 1500°C , by the Hf–Ta–Si–O surface layer. Here HfSiO_4 and Ta_xO_y increase the oxide film viscosity and create “pinning points”, which change the direction of crack propagation or inhibit it [57].

Ren X. et al. [59] reported that a two-layer $\text{Ta}_x\text{Hf}_{1-x}\text{B}_2$ –SiC/SiC multiphase coating $120\text{--}190\text{ }\mu\text{m}$ thick protects C/C composites from oxidation in air at $t = 1500^\circ\text{C}$ for more than 1480 h, and from ablation, for 40 s at the 1927°C oxyacetylene flame temperature. The number of cracks and holes after oxidation was relatively small, when compared to the SiC/SiC coating, and the glassy layer surface contained Ta and Hf oxidation products indicating the formation of a multiphase silicate glass. The melting point of tantalum and hafnium oxides is higher than that of SiO_2 , so adding these components to the glass increases its thermal stability and viscosity for better ablation and oxidation resistance through the synergistic effect of the multiphase oxides [59].

The presence of the $\text{Zr}_x\text{Ta}_{1-x}\text{B}_2$ solid solution in the SiC coating significantly improves its oxidation protection properties. Ren X. et al. [60] reported that after oxidation at $t = 1500^\circ\text{C}$ for 1412 h, the weight loss of a C/C composite coated with $\text{Zr}_x\text{Ta}_{1-x}\text{B}_2$ –SiC/SiC was only 0.1 wt. %, while for the ZrB_2 –SiC/SiC coating, it was 0.22 wt. % for 550 h. The TGA showed the coating is resistant to oxidation

in a wide temperature range (from room temperature to 1500 °C). The coated C/C composite weight gain at the end of the test was 1.8 wt. % (C/C composites with $\text{ZrB}_2\text{--SiC/SiC}$ and $\text{TaB}_2\text{--SiC--Si/SiC}$ coatings lost 10.3 and 11.2 wt. %) [60]. Ren X. et al. explained the high oxidation resistance of the $\text{Zr}_x\text{Ta}_{1-x}\text{B}_2\text{--SiC/SiC}$ coating by the formation of a heterogeneous Zr--Ta--Si--O glass layer on its surface (containing evenly distributed Zr and Ta oxides forming an “inlaid structure” providing cracks deflection and elimination), as well as by the synergistic effect of multiple protective mechanisms provided by the coating components.

Tong K. et al. [61] studied the ablation resistance of a multiphase Zr--Ta--B--SiC coating with various Zr/Ta weight ratios on a C/C composite at $t = 2300$ °C. Adding Ta led to the formation of the $(\text{Zr, Ta})\text{B}_2$ solid solution, relieving thermal stress during the synthesis and removes the layer defects. Ta also had a noticeable effect on the composition and morphology of the coating after ablation. Tong K. et al. [61] also reported that the $\text{Zr}_{0.7}\text{Ta}_{0.3}\text{B}_2\text{--SiC}$ coating has better ablation resistance due to the formation of a thermal barrier and low volatility of the Zr--Ta--O layer. Furthermore, the Ta–O bond stabilizes the high-temperature $t\text{--ZrO}_2$ phase. The samples with low Ta (~10 mol. %) and excessive Zr contents in the solid solution after ablation showed the formation of multiple nanosized Zr--Ta--O nuclei, thus making it impossible to form a homogeneous layer over the glass phase and to increase its viscosity. That is, SiO_2 was still exposed directly to the plasma generator flame and intensively evaporated during the ablation. When Ta is in excess (~70 mol. %), the ablation results in the extensive formation of the liquid Zr--Ta--O phase with low viscosity, rapidly exposing the surface. At the same time, gaseous SiO , CO , CO_2 and B_2O_3 compounds volatilized making numerous pores and holes in the glassy layer as channels for oxygen diffusion [61].

2.2. $\text{ZrB}_2\text{--SiC}$ coatings alloyed with complex tantalum carbide

The Ta_4HfC_5 complex tantalum-hafnium carbide seems suitable for high-temperature applications with its properties [29; 30]. However, it cannot protect C/C composites from oxygen due to its low heat resis-

tance [62]. Therefore, it was proposed to apply a 2-layer coating. The inner layer is Ta_4HfC_5 and the outer layer is $\text{ZrB}_2\text{--SiC--Ta}_4\text{HfC}_5$. Such a coating can be efficient to protect C/C composites from oxidation at high temperatures. The weight loss of the coated samples during isothermal oxidation tests at $t = 1500$ °C for 20 h was 3.3 %. The weight loss after ten 1500 °C to 20 °C thermal cycles with a 10 min isothermal holding at the max temperature was 9.5 %, indicating the high heat resistance and thermal stability of the coating.

The gas-tight, continuous silicate glass layer containing ZrO_2 , SiO_2 , ZrSiO_4 , Ta_2O_5 and HfO_2 particles has a low oxygen diffusion rate and a relatively high self-healing ability. Nevertheless, the pores and microcracks resulting from the different thermal expansion coefficients of the coating and substrate, and from the gaseous oxidation products release, are the primary cause of weight loss. They also adversely affect the protective performance of the coating.

2.3. $\text{ZrB}_2(\text{HfB}_2)\text{--SiC}$ coatings alloyed with tantalum silicides

Since the SiC thermal expansion coefficient is low, replacing it with another stable SiO_2 source would increase the protective performance of $\text{ZrB}_2(\text{HfB}_2)\text{--SiC}$ coatings at temperatures above 1700 °C. Adding more components may increase the glass phase viscosity and improve the oxidation resistance of the coating.

When added to $\text{HfB}_2\text{--SiC--TaSi}_2$ coatings, the passivating power of TaSi_2 inhibits the intense oxidation of SiC at $t = 1700$ °C. The expansion caused by the TaSi_2 oxidation slows the disintegration of HfB_2 and increases the coatings structural resistance to oxidation. The addition of tantalum disilicide also leads to the formation of a heterogeneous Hf--Ta--B--Si--O high-viscosity glass layer, which reduces the oxygen permeability of the coating from 4.87 % to 0.31 % [63]. It was shown that the optimal TaSi_2 content has a positive effect and seems promising for alloying $\text{HfB}_2\text{--SiC}$ coatings. Adding 20 wt. % of TaSi_2 slows down the coating removal rate by improving its gas tightness, while an excessive amount of TaSi_2 reduces the oxidation protection performance.

Tantalum disilicide is also used to improve the ablation resistance of $\text{ZrB}_2\text{--SiC}$ coatings on C/C composites.

Adding 10 vol. % of TaSi_2 to a ZrB_2 –27 vol. % SiC coating results in the porosity drop from 16.65 to 9.65 %, better mechanical properties, and ablation resistance at $t = 2000^\circ\text{C}$ for 10 min [64]. The effect of TaSi_2 on the resistance to high-temperature gas corrosion was investigated at $t = 1700^\circ\text{C}$ in the air for 30 min. A ZrB_2 –20 vol. % SiC–10 vol. % TaSi_2 coating on siliconized graphite lasts much longer than a TaSi_2 -free coating. This indicates a higher heat resistance of the former, due to the formation of a tantalum-containing oxide layer with a significantly lower oxygen permeability [65]. The ZrB_2 –20 vol. % SiC–10 vol. % TaSi_2 oxide coating layer is significantly thinner than the ZrB_2 –20 vol. % SiC coating. Despite the absence of pores and bubbles (the TaSi_2 -free coating has multiple defects), cracking was observed.

In order to improve the overall performance of the coating, Ren Y. et al. [66] studied the effect of additional silicon vapor infiltration as the coating is formed. The resulting ZrB_2 –SiC– TaSi_2 –Si coating on siliconized graphite efficiently protects the material from oxidation for 300 h at $t = 1500^\circ\text{C}$ in stagnant air. The oxidation did not cause any cracking or delamination. Ren Y. et al attributed this to the modified coating structure with a dense ZrB_2 –SiC– TaSi_2 primary layer under an additional silicon layer. The coating can withstand severe thermal cycling from 20 to 1500°C (20 cycles). The area of the cracks per unit of surface area was only $3.8 \cdot 10^{-3}$, which indicates good thermal resistance due to the self-healing of the surface cracks. Tables 3 and 4 list some oxidation and ablation resistance properties of the coatings.

Table 3. Oxidation resistance of carbon materials with $\text{ZrB}_2(\text{HfB}_2)$ –SiC coatings alloyed with tantalum compounds

Таблица 3. Характеристики окислительной стойкости углеродных материалов с покрытиями на основе керамики $\text{ZrB}_2(\text{HfB}_2)$ –SiC, модифицированной соединениями тантала

Coating	Substrate	Manufacturing process	Oxidation conditions	Phase composition after oxidation	Weight change	Reference
ZrB_2 –SiC– $\text{Ta}_4\text{HfC}_5/\text{Ta}_4\text{HfC}_5$	2D C/C	Slip molding/pack cementation	1500°C , 20 h	ZrO_2 , Ta_2O_5 , ZrSiO_4 , SiO_2 , HfO_2 , SiC	–3.3 %	[62]
ZrB_2 –SiC– TaSi_2 –Si/SiC	Graphite	Slip molding + Si vapor infiltration/pack cementation	1500°C , 300 h	SiO_2 , ZrB_2 , SiC	4.76 mg/cm ²	[66]
$(\text{ZrTa})\text{B}_2$ –SiC–Si	Graphite	Slip molding + Si vapor infiltration	1500°C , 347 h	$(\text{Zr, Ta})\text{B}_2$, SiO_2	0.33 %	[56]
$\text{Zr}_x\text{Ta}_{1-x}\text{B}_2$ –SiC/SiC	2D C/C	<i>In situ</i> reaction synthesis/pack cementation	1500°C , 1412 h	ZrO_2 , Ta_2O_5 , ZrSiO_4 , SiO_2 , $\text{Ta}_2\text{O}_{2.2}$, SiC	–0.1 %	[60]
$\text{Ta}_x\text{Hf}_{1-x}\text{B}_2$ –SiC/SiC	2D C/C	<i>In situ</i> reaction synthesis/pack cementation	1500°C , 1480 h	HfO_2 , TaO_2 , HfSiO_4 , SiO_2 , TaO , $\text{Ta}_{0.8}\text{O}_2$, Ta_2O , SiC	–2,8 mg/cm ²	[59]
$\text{Hf}_{0.5}\text{Ta}_{0.5}\text{B}_2$ –SiC–Si	Graphite	Impregnation and pyrolysis + reactive Si gas infiltration	1500°C , 2080 h	$\text{Hf}_{0.5}\text{Ta}_{0.5}\text{B}_2$, Ta_2O_5 , HfSiO_4 , SiO_2	1.74 %	[57]
$\text{Ta}_{0.5}\text{Zr}_{0.5}\text{B}_2$ –Si–SiC	Graphite	Slip molding + <i>in situ</i> reactive synthesis	1650°C , 70 h	SiO_2	–0.56 %	[55]
ZrB_2 –20 vol. % SiC–10 vol. % TaSi_2 /SiC	Graphite	Slip molding/pack cementation	1700°C , 30 min	ZrO_2 , ZrSiO_4 , SiO_2 , TaC	3.81 mg/cm ²	[65]
HfB_2 –20 wt. % SiC–20 wt. % TaSi_2	Graphite	SPS	1700°C , 100 min	HfO_2 , $\text{Ta}_2\text{O}_{2.2}$, HfSiO_4 , SiO_2	~15 mg/cm ²	[63]

Table 4. Ablation resistance of carbon materials coated with $ZrB_2(HfB_2)$ –SiC ceramics alloyed with tantalum compounds

Таблица 4. Характеристики стойкости к абляции углеродных материалов с покрытиями на основе керамики $ZrB_2(HfB_2)$ –SiC, модифицированной соединениями тантала

Coating	Flame test conditions				Mass ablation rate, mg/s	Linear ablation rate, μm/s	Reference
	t , °C	Time, s	Flow rate, l/s				
			O ₂	C ₂ H ₂			
Ta _x Hf _{1-x} B ₂ -SiC/SiC	1927	40	0.2–0.3	0.1–0.2	1.590	3.21	[59]
ZrB ₂ -SiC-TaSi ₂	2000	600	0.72	0.25	0.114	–	[64]
Hf _{0.5} Ta _{0.5} B ₂ -SiC-Si	2130	60	0.244	0.167	1.050	-10.20	[57]
(Zr _{0.7} Ta _{0.3})B ₂ -SiC	2300	120	0.42	0.31	0.033	3.01	[61]
Ta _{0.5} Zr _{0.5} B ₂ -Si-SiC	2.4 MW/m ² *	60	0.24	0.18	0.150	0.35	[55]
	4.2 MW/m ² *	40	0.42	0.31	4.900	3.25	
* Heat flux was reported instead of the flame temperature.							

* Heat flux was reported instead of the flame temperature.

3. Carbon-ceramic composites with a (C)–SiC– ZrB_2 matrix alloyed with tantalum compounds

In the last decade, many researchers studied high-temperature composites with a ceramic matrix, since solid UHTCs are inherently brittle and lack sufficient resistance to thermal shock [2]. Reinforcing fibers increase the strength of the composite, and adapt its mechanical and thermal properties to the specific application. Carbon-ceramic composites (C/SiC) reinforced with continuous carbon fibers overcome the inherent brittleness and low thermal resistance of UHTCs offering better thermal performance and increased ablation resistance [1].

Kannan R. et al. [67] showed that adding 20 wt. % of Ta to the C/SiC– ZrB_2 composite leads to the Ta_xC_y formation from the residual carbon and increases the ablation resistance due to stabilization of the t - ZrO_2 martensitic phase and the low melting point of Ta_xC_y capable of enveloping the ZrO_2 matrix particles and reducing the anionic conductivity at $t \geq 2000$ $^{\circ}\text{C}$. Kannan R. et al. [67] also attributed the higher ablation resistance to the low thermal conductivity of the Zr–Ta–Si–O oxide layer which inhibits the heat transfer from the surface inside the composite, and to the relatively high bond strength between the carbon fibers and the matrix due to the presence of residual metallic Ta.

Li L. et al. [68] reported that adding 24 vol. % of tantalum carbides into the matrix also resulted in higher

ablation resistance of C/SiC– ZrB_2 –TaC 2D composites due to the oxidation and formation of liquid Ta_2O_5 (at $t > 1870$ $^{\circ}\text{C}$) capable of healing cracks during ablation and retaining the loose ZrO_2 , building a gastight layer around the fibers. It was concluded that the TaC content should be increased, and the substance should be more evenly distributed across the matrix to further improve the ablation resistance of such composites.

C/SiC composites alloyed with ZrB_2 and TaC showed higher flexural strength (up to 27 %), Young's modulus (up to 28 %), and interlayer shear strength (up to 22 %). Uhlmann F. et al. [69] attributed the latter to the addition of TaC. The thermochemical stability of the C/SiC– ZrB_2 –TaC composites under the combustion chamber conditions (exposure to a hot gas for 15 min, 1725–1860 $^{\circ}\text{C}$ measured surface temperature) improved, while the oxygen permeability significantly decreased. The reason for this is that the oxide film in the Si–Zr–Ta–O system is a diffusion barrier, preventing the penetration of combustion products into the underlying layers and protecting them from further oxidation [69].

For the C/C–2SiC–1 ZrB_2 –2TaC composite (the numbers are the relative volumes of the ceramic particles) the ablation properties deteriorated which may be a result of the TaC addition. The higher ablation rate (Table 5) is attributed to the formation of the Ta_2O_5 liquid phase subject to strong mechanical removal and erosion at $t = 2700 \pm 300$ $^{\circ}\text{C}$ [70].

Table 5. Ablation resistance of the C/SiC composite with the (C)–SiC– ZrB_2 matrix alloyed with tantalum carbideТаблица 5. Характеристики стойкости к абляции УККМ с матрицей на основе (C)–SiC– ZrB_2 , легированной карбидом тантала

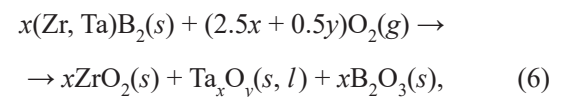
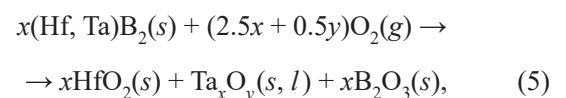
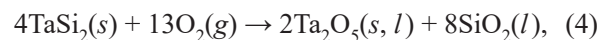
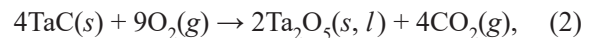
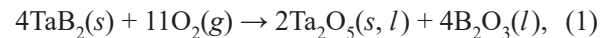
C/SiC composite	Manufacturing process	Density, g/cm ³	Porosity, %	Flame test conditions				Mass ablation rate, mg/s	Linear ablation rate, μm/s	Reference
				<i>t</i> , °C	Time, s	Gas pressure/flow rate				
						O ₂	C ₂ H ₂			
C/SiC–ZrB ₂ –Ta _{<i>x</i>} C _{<i>y</i>}	Reactive HP/impregnation and pyrolysis	2.82	21.0	1600	120	0.4 MPa	0.01 MPa	1.33	0.19	[67]
					600			0.02	0.27	
				1800	120			1.80	0.25	
					600			0.47	0.63	
				2000	120			3.05	0.39	
					600			2.19	1.43	
C/C–2SiC–1ZrB ₂ –2TaC	Powder infiltration + isothermal vapor infiltration	–	–	2700±300	30	1.36 m ³ /h	1.04 m ³ /h	~59	–	[70]
2D C/SiC–ZrB ₂ –TaC	Vapor infiltration + slip molding	2.35	11.5	3000	20	0.4 MPa; 1.51 m ³ /h	0.095 MPa; 1.12 m ³ /h	–	26	[68]

4. Mechanisms improving the oxidation and ablation resistance of $\text{ZrB}_2(\text{HfB}_2)$ –SiC composites alloyed with tantalum compounds

UHTC oxidation and ablation performance is largely determined by the oxidation product properties, and the surface chemical and physical processes occurring in oxygen-containing environments. Consequently, modifications to the oxide film's chemical composition and structure can improve the resistance to high-temperature oxidation and ablation. Opeka M. et al. [7] noted that UHTC composites during the oxidation of which synthesize relatively refractory glass layers with low oxygen diffusion rates and high self-healing ability are potentially heat-resistant materials. For several reasons discussed below, alloying with tantalum compounds modifies the oxide film and improves the oxidation and ablation resistance.

4.1. Phase separation in the oxide surface layer

Oxidation of tantalum-containing components in UHTC composites can be represented by the following reactions:



where s , l and g denote the aggregate state of the phases: solid, liquid, and gaseous.

As can be seen the relatively refractory Ta_2O_5 is formed ($t_{\text{melt}} = 1882^\circ\text{C}$ [10]). The presence of group IV–VI transition metal oxides (e.g., tantalum) in borosilicate glass causes intense phase separation (immiscibility) of the glass phase. It increases the heat resistance of $\text{ZrB}_2(\text{HfB}_2)$ –SiC composites by increasing the liquidus temperature and viscosity [20; 21; 27; 38; 44; 55; 56; 59; 60; 65]. Higher viscosity, in turn, reduces the oxygen diffusion rate through the film. According

to the Stokes-Einstein relation, the diffusion coefficient is inversely proportional to viscosity [71]:

$$D = \frac{kT}{6\pi\eta r}, \quad (7)$$

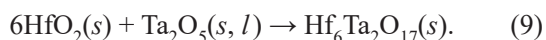
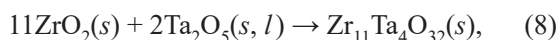
where D is the diffusion coefficient, k is the Boltzmann constant, T is the temperature, η is the solution viscosity, and r is the average radius of the diffusing particles.

Zhang M. et al. [63] showed that $\text{Hf}^{4+}/\text{Ta}^{5+}$ transition metal cations interact with the silica-oxygen tetrahedral lattice $[\text{SiO}_4]$ forming 3D ionic clusters. This increases the glass viscosity and reduces the oxygen mass transfer. Zhang M. et al. [63] showed that refractory hafnium and tantalum oxide particles distributed in a viscous-fluid glass layer improve heat resistance by increasing the number of barriers to oxygen movement. This significantly limits its diffusion rate through the oxide film.

Eakins E. et al. [15], Peng F. et al. [21] and Thimmappa S. et al. [44] observed a decrease in the porosity of the oxide layer under the surface glass layer. This was attributed to the higher viscosity of the glass phase containing tantalum, which is less mobile reducing the capillary rise from the lower layers. Borosilicate glass enriched with tantalum also prevents cracking and heals defects [27; 38; 64; 67; 69]. Also, the higher viscosity and liquidus temperature contribute to the partial suppression of boron evaporation from glass [7].

4.2. Formation of refractory solid solutions and complex oxides

Partial dissolution of tantalum in the zirconium or hafnium boride can result in the formation of a solid solutions which oxidizes to Zr-Ta-O and Hf-Ta-O solid solutions when exposed to oxygen [38; 44]. The reaction between the $\text{ZrO}_2(\text{HfO}_2)$ и Ta_2O_5 phases produces the $\text{Zr}_{11}\text{Ta}_4\text{O}_{32}$ ($\text{Zr}_{2.75}\text{TaO}_8$) [55] zirconium-tantalum oxides or the $\text{Hf}_6\text{Ta}_2\text{O}_{17}$ [72] hafnium-tantalum oxides, e.g.:

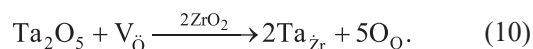


The refractory solid solutions and/or complex oxides in the films enhance resistance to oxidation and ablation without inducing additional thermal

stress. The mechanical and thermophysical properties of solid solutions are easier to control compared to stoichiometric phases [61]. Hu C. et al. [34] proposed that the formation of a solid solution reduces the activation energy of the boride grain boundaries, contributing to the formation of coherent structures. The $\text{Zr}_{11}\text{Ta}_4\text{O}_{32}$ и $\text{Hf}_6\text{Ta}_2\text{O}_{17}$ phases act as barriers in the oxygen-acetylene flame preventing the erosive removal of the internal layers by the high-speed gas flows due to the low thermal conductivity and relatively high refractoriness of these phases [55; 67; 72]. The heterogeneous structure of the oxide film hampers cracking and crack propagation [38].

4.3. Reducing the oxygen vacancies concentration in the $\text{ZrO}_2(\text{HfO}_2)$ lattice

Compositions that reduce oxygen transport through the ZrO_2 and HfO_2 matrix phases also increase heat resistance [7]. ZrO_2 and HfO_2 oxides become non-stoichiometric as oxygen vacancies are formed in the lattices under the low partial pressure of oxygen (e.g., under a gastight borosilicate glass layer) or due to the addition of lower valence cations (Y^{3+} , La^{3+} , etc.) [8]. The partial replacement of Zr^{4+} and Hf^{4+} with Ta^{5+} decreases the concentration of oxygen vacancies according to the Kreger-Wink reaction [26]. The reaction for the ZrO_2 lattice doping is



A decrease in the oxygen vacancy concentration reduces the anionic conductivity and decreases the oxidation rate of $\text{ZrB}_2(\text{HfB}_2)\text{-SiC}$ composites [26; 65].

4.4. Inhibition of $\text{ZrO}_2(\text{HfO}_2)$ polymorphic transformations

The substitution of Zr^{4+} and Hf^{4+} for Ta^{5+} in the $\text{ZrO}_2(\text{HfO}_2)$ lattice depletes the oxygen vacancies and partially stabilizes the lattice [67]. This reduces the rate of the diffusion-free martensitic tetragonal-to-monoclinic phase transformation. It also decreases the volume expansion associated with the transformation and the possibility of cracking in the oxide film during thermal cycling [8; 21; 66]. This factor improves the performance of composites exposed to high temperatures, reducing the oxide film cracking and increasing its adhesion and cohesion [61].

4.5. Changing the oxide layer microstructure

The effect of tantalum on the oxide particle size in the glass phase also affects the oxidation processes. Peng F. et al. [22] reported that the size of zirconium dioxide particles decreases when TaB_2 is added. The resulting borosilicate glass phase has a greater tendency to be captured by the lower oxide sublayers containing dispersed particles. It makes these layers more impermeable to atmospheric oxygen and improves the overall heat resistance of the material.

Tong K. et al. [61] also found that by increasing the tantalum compound content in UHTCs, the morphology of the synthesized complex oxide in the Zr–Ta–O system changes from dispersed nuclei to sintered rod-like grains. It improves the ablation resistance, since this oxide works as a “pinning” phase for efficient retention of glassy SiO_2 and resistance to mechanical erosion. Similarly, the formation of a heterogeneous oxide film in the Hf–Ta–Si–O system from the immiscible HfSiO_4 and Ta_xO_y phases of the silicate glass increases the surface layer viscosity and creates “pinning points”, inhibiting or eliminating cracking [57]. It reduces the probability of crack penetration through the oxide film and improves heat resistance [59].

5. Reduction mechanisms of oxidation and ablation resistance in $\text{ZrB}_2(\text{HfB}_2)$ –SiC composites alloyed with tantalum compounds

Along with the noted improvement in heat-resistant and anti-ablation properties when alloying $\text{ZrB}_2(\text{HfB}_2)$ –SiC composites with tantalum compounds, under certain conditions these positive effects are limited, and, in some cases, oxidation and ablation resistance even deteriorates. Some studies report negative effects of tantalum compounds on the HfB_2 –SiC system [26; 35], at temperatures above 1700 °C [24; 26; 39], and with improper concentrations [22; 27; 39].

The reasons for the oxidation and ablation resistance deterioration are listed below.

5.1. Formation of low-viscosity liquid phases

Adding tantalum may have a negative effect on the oxidation of $\text{ZrB}_2(\text{HfB}_2)$ –SiC composites at temperatures above 1650 °C, since the presence of Ta_2O_5 in the oxide film reduces its heat resistance due to the formation of liquid phases [8; 24; 37].

High tantalum content (~70 mol. %) results in the extensive formation of the low-viscosity liquid phase during ablation. It causes intensive oxide film removal, holes, and bare areas on the surface [61].

Opila E. et al. [39] also observed the formation of a significant amount of the liquid phase (a mixture of oxiboride, silicate, and zirconate phases) during the oxidation of ZrB_2 –20 vol. % SiC–20 vol. % TaSi_2 at $t = 1927$ °C, which was the key reason for the deterioration of its heat resistance [39].

5.2. Damage of frame structures in the oxide layer

The presence of Ta_2O_5 in the film at temperatures above 1700 °C leads to the formation of the $\text{Zr}_{11}\text{Ta}_4\text{O}_{32}$ or $\text{Hf}_6\text{Ta}_2\text{O}_{17}$ complex oxides. It reduces the heat resistance of the mechanical framework based on $\text{ZrO}_2(\text{HfO}_2)$, accelerating the oxidation and reducing the ablation resistance [22; 24].

Due to the limited solubility of tantalum in the ZrO_2 thermally grown *in situ* its excess forms the low-melting oxide phases, from which zirconium dioxide crystallizes contributing to the formation of dendrites [39]. Dendrite growth from the oxide sublayer to the glass surface increases the overall oxidation rate, since the dendrites act as anion channels. Another reason is the poor wetting of the dendrites with the glass phase, which contributes to increased oxygen penetration through the phase interfaces [22].

5.3. Structural changes in the oxide layer leading to porosity and cracking

The formation of Ta_2O_5 inside the ZrO_2 grains leads to a large volume expansion exceeding 50 % of the initial one. It causes irreversible damage to the ZrO_2

grains, including their cracking from the inside. This disturbs the compactness and continuity of the oxide layers and increases the mass transfer rate across the oxide film [37]. Silvestroni L. et al. [37] also noted that the platelet-shaped formations of the mixed $Zr_{2.75}TaO_8$ oxide turn vertical at $t = 1650$ °C. This configuration has extra channels for oxygen diffusion due to a significant increase in the platelets-glass phase interface surface area, which negatively affects the UHTC heat resistance.

Opila E. et al. [26] reported that adding tantalum carbides to ZrB_2 -SiC reduces the oxidation resistance, since a porous oxide layer is formed due to the release of gaseous CO and/or CO_2 oxidation products. The structure discontinuity leads to accelerated oxidation, since the gas phase mass transfer through the cracks and pores (even at the Knudsen diffusion mode) is much easier than diffusion in condensed phases [24].

5.4. Changes to the oxidation mechanism

Alloying ZrB_2 -SiC ceramic composites with tantalum may change the processes governing its oxidation. Wang Y. et al. [27] suggested that the mass transfer of tantalum and/or silicon cations diffusing from the substrate to the oxide film during formation of the SiC-TaC depleted layer, is crucial. At low tantalum concentrations (~10 vol. %) most of the Ta_2O_5 dissolves in ZrO_2 forming a solid solution. The remainder is insufficient to seal the porous zirconium dioxide layer, resulting in a loose structure not protected by SiO_2 and/or $ZrSiO_4$ gastight layers, and a significant increase in the UHTC oxidation rate [27].

The estimated activation energy of the silicon diffusion to the surface through the oxide layer is 315 kJ/mol. It is much higher than the previously reported values for the inward oxygen diffusion (120–140 kJ/mol [73]). This indicates the key contribution of the outward tantalum diffusion, than the inward oxygen diffusion.

5.5. Increasing the coating thermal expansion coefficient

Cracks in UHTC coatings may be caused by the difference in the substrate and coating thermal expansion coefficients [65]. The thermal expansion coefficient

of tantalum compounds is higher than that of $ZrB_2(HfB_2)$ or SiC [63]. Oxidation induces compression forces in the coating, but rapid cooling leads to tensile stresses and easy cracking in the oxide layer [65]. Increasing the $TaSi_2$ content leads to heat resistance deterioration as penetrating cracks occur [63].

Conclusion

We reviewed the available studies of tantalum alloying effects on the structure and resistance to high-temperature oxidation and ablation of $ZrB_2(HfB_2)$ -SiC UHTCs. The studies discuss different materials: bulk ceramics, heat-resistant coatings on C/C composites and graphite, and C/C composites with a UHTC matrix. It is shown that alloying with Ta-containing components may have both positive and negative effects. The increase in heat and ablation resistance is primarily caused by:

- higher viscosity and thermal stability of the borosilicate glass containing zirconium (hafnium) and tantalum cations;
- anionic conductivity reduction and partial stabilization of the $ZrO_2(HfO_2)$ lattice due to tantalum doping;
- compaction and sintering of the oxide sublayer containing $ZrO_2(HfO_2)$ and $ZrSiO_4(HfSiO_4)$ grains;
- formation of temperature-resistant complex oxides like $Zr_{11}Ta_4O_{32}$ or $Hf_6Ta_2O_{17}$ on the surface.

The key reasons for the negative effect of alloying are:

- poor oxide film continuity as the $ZrO_2(HfO_2)$ grains are damaged by the TaB_2 oxidation or a significant gas release during the TaC oxidation;
- the emergence of additional oxygen diffusion channels as the $Zr_{11}Ta_4O_{32}$ or $Hf_6Ta_2O_{17}$ platelets turn vertical;
- an increase of the liquid phase share subjected to mechanical removal by high-speed gas flows.

The effects of alloying are not so unambiguous: there are limitations in terms of concentration, structure, and temperature. The oxidation and ablation resistance and the mechanisms governing the UHTC behaviors are different for various alloying components and ambient conditions. Consequently, both positive and negative aspects should be considered when selecting the type

and amount of alloying tantalum, as well as to determine whether one or another factor is decisive under given oxidation/ablation conditions.

References / Список литературы

- Ni D., Cheng Y., Zhang J., Liu J.X., Zou J., Chen B., Wu H., Li H., Dong S., Han J., Zhang X., Fu Q., Zhang G.J. Advances in ultra-high temperature ceramics, composites, and coatings. *Journal of Advanced Ceramics*. 2022;11(1):1–56. <https://doi.org/10.1007/s40145-021-0550-6>
- Binner J., Porter M., Baker B., Zou J., Venkatachalam V., Rubio Diaz V., D'Angio A., Ramanujam P., Zhang T., Murthy T.S.R.C. Selection, processing, properties and applications of ultra-high temperature ceramic matrix composites, UHTCMCs: a review. *International Materials Reviews*. 2020;65(7):389–444. <https://doi.org/10.1080/09506608.2019.1652006>
- Ultra-high temperature ceramics: materials for extreme environment applications (Ed. by W.G. Fahrenholtz, E.J. Wuchina, W.E. Lee, Y. Zhou). Hoboken, New Jersey: John Wiley & Sons, Inc., 2014. 464 p.
- Justin J.-F., Julian-Jankowiak A., Guérineau V., Mathivet V., Debarre A. Ultra-high temperature ceramics developments for hypersonic applications. *CEAS Aeronautical Journal*. 2020;11:651–664. <https://doi.org/10.1007/s13272-020-00445-y>
- Simonenko E.P., Sevast'yanov D.V., Simonenko N.P., Sevast'yanov V.G., Kuznetsov N.T. Promising ultra-high-temperature ceramic materials for aerospace applications. *Russian Journal of Inorganic Chemistry*. 2013;58(14):1669–1693. <https://doi.org/10.1134/S0036023613140039>
- Tang S., Hu Ch. Design, preparation and properties of carbon fibers reinforced ultra-high temperature ceramic composites for aerospace applications: a review. *Journal of Materials Science & Technology*. 2017;33(2):117–130. <https://doi.org/10.1016/j.jmst.2016.08.004>
- Opeka M.M., Talmy I.G., Zaykoski J.A. Oxidation-based materials selection for 2000 °C + hypersonic aerosurfaces: Theoretical considerations and historical experience. *Journal of Materials Science*. 2004;39:5887–5904. <https://doi.org/10.1023/B:JMSC.0000041686.21788.77>
- Levine S.R., Opila E.J. Tantalum addition to zirconium diboride for improved oxidation resistance. *NASA/TM-2003-212483*. 2003.
- CRC Handbook of Chemistry and Physics 85th edition. (Ed. by D.R. Lide). CRC Press, Boca Raton, FL. 2005. 2661 p.
- Springer Handbook of condensed matter and materials data (Ed by W. Martienssen, H. Warlimont). Heidelberg: Springer, 2005. 1120 p.
- Schmidt F.F. Tantalum and tantalum alloys. DMIC Report 133/OTS PB 151091. 1960. 328 p.
- Mai Z., Zhang X., Liu Y., Yu H., Wang F. Insight into the structure dependence on physical properties of the high temperature ceramics TaB_2 boride. *Vacuum*. 2020;177:109427 <https://doi.org/10.1016/j.vacuum.2020.109427>
- Schlesinger M.E. The Si-Ta (silicon-tantalum) system. *Journal of Phase Equilibria*. 1994;15:90–95. <https://doi.org/10.1007/BF02667688>
- Zhang X., Hilmas G.E., Fahrenholtz W.G. Synthesis, densification, and mechanical properties of TaB_2 . *Materials Letters*. 2008;62(27):4251–4253. <https://doi.org/10.1016/j.matlet.2008.06.052>
- Lee S.J., Kim D.K. Effect of TaB_2 addition on the oxidation behaviors of ZrB_2 -SiC based ultra-high temperature ceramics. *Korean Journal of Materials Research*. 2010;20(4):217–222. <https://doi.org/10.3740/MRSK.2010.20.4.217>
- Eakins E., Jayaseelan D.D., Lee W.E. Toward oxidation-resistant ZrB_2 -SiC ultra high temperature ceramics. *Metallurgical and Materials Transactions A*. 2011;42:878–887. <https://doi.org/10.1007/s11661-010-0540-8>
- Monteverde F., Savino R. Stability of ultra-high-temperature ZrB_2 -SiC ceramics under simulated atmospheric re-entry conditions. *Journal of the European Ceramic Society*. 2007;27:4797–4805. <https://doi.org/10.1016/j.jeurceramsoc.2007.02.201>
- Bundschuh K., Schütze M. Materials for temperatures above 1500 °C in oxidizing atmospheres. Part I: Basic considerations on materials selection. *Materials and Corrosion*. 2001;52(3):204–212. [https://doi.org/10.1002/1521-4176\(200103\)52:3<204::AID-MACO204>3.0.CO;2-J](https://doi.org/10.1002/1521-4176(200103)52:3<204::AID-MACO204>3.0.CO;2-J)
- Zhang X., Hu P., Hun J., Meng S. Ablation behavior of ZrB_2 -SiC ultra high temperature ceramics under simulated atmospheric re-entry conditions. *Composites Science and Technology*. 2008;68(7-8):1718–1726. <https://doi.org/10.1016/j.compscitech.2008.02.009>
- Talmy I.G., Zaykoski J.A., Opeka M.M., Dallek S. Oxidation of ZrB_2 ceramics modified with SiC and group IV–VI transition metal diborides. In: *Proceedings of the International Symposium «High Temperature Corrosion and Materials Chemistry III»* (Eds. M. McNallan, E. Opila). The Electrochemical Society, Inc., Pennington, NJ. 2001;12:144–158.
- Peng F., Speyer R.F. Oxidation resistance of fully dense ZrB_2 with SiC, TaB_2 , and $TaSi_2$ additives. *Journal of the American Ceramic Society*. 2008;91(5):1489–1494. <https://doi.org/10.1111/j.1551-2916.2008.02368.x>
- Peng F., Berta Y., Speyer R.F. Effect of SiC, TaB_2 and $TaSi_2$ additives on the isothermal oxidation resistance of fully dense zirconium diboride. *Journal of Materials Research*. 2009;24(5):1855–1867. <https://doi.org/10.1557/jmr.2009.0216>
- Peng F., Van Laningham G., Speyer R.F. Thermogravimetric analysis of the oxidation resistance of ZrB_2 -SiC and ZrB_2 -SiC- TaB_2 -based compositions in the 1500–1900 °C range. *Journal of Materials Research*. 2011;26(1):96–107. <https://doi.org/10.1557/jmr.2010.38>
- Hu P., Zhang X.H., Han J.C., Luo X.G., Du S.Y. Effect of various additives on the oxidation behavior of ZrB_2 -based ultra-high-temperature ceramics at 1800 °C. *Journal of the American Ceramic Society*. 2010;93(2):345–349. <https://doi.org/10.1111/j.1551-2916.2009.03420.x>
- Mohammadzadeh B., Jung S., Lee T.H., Le Q.V., Cha J.H., Jang H.W., Lee S.H., Kang J., Shokouhimehr M. Manufacturing ZrB_2 -SiC-TaC composite: potential application for aircraft wing assessed by frequency analysis through

- finite element model. *Materials*. 2020;13(10):2213. <https://doi.org/10.3390/ma13102213>
26. Opila E., Levine S., Lorincz J. Oxidation of ZrB₂- and HfB₂-based ultra-high temperature ceramics: Effect of Ta additions. *Journal of Materials Science*. 2004;39:5969–5977. <https://doi.org/10.1023/B:JMSC.0000041693.32531.d1>
 27. Wang Y., Ma B., Li L., An L. Oxidation behavior of ZrB₂-SiC-TaC ceramics. *Journal of the American Ceramic Society*. 2012;95(1):374–378. <https://doi.org/10.1111/j.1551-2916.2011.04945.x>
 28. Kakroudi M.G., Alvari M.D., Asl M.S., Vafa N.P., Rabizadeh T. Hot pressing and oxidation behavior of ZrB₂-SiC-TaC composites. *Ceramics International*. 2020;46(3):3725–3730. <https://doi.org/10.1016/j.ceramint.2019.10.093>
 29. Simonenko E.P., Simonenko N.P., Lysenkov A.S., Sevast'yanov V.G., Kuznetsov N.T. Reactive hot pressing of HfB₂-SiC-Ta₄HfC₅ ultra-high temperature ceramics. *Russian Journal of Inorganic Chemistry*. 2020;65:446–457. <https://doi.org/10.1134/S0036023620030146>
 30. Simonenko E.P., Simonenko N.P., Gordeev A.N., Kolesnikov A.F., Chaplygin A.V., Lysenkov A.S., Nagornov I.A., Sevastyanov V.G., Kuznetsov N.T. Oxidation of HfB₂-SiC-Ta₄HfC₅ ceramic material by a supersonic flow of dissociated air. *Journal of the European Ceramic Society*. 2021;41(2):1088–1098. <https://doi.org/10.1016/j.jeurceramsoc.2020.10.001>
 31. McCormack S.J., Tseng K., Weber R.J.K., Kapush D., Ushakov S.V., Navrotsky A., Kriven W.M. In-situ determination of the HfO₂-Ta₂O₅-temperature phase diagram up to 3000 °C. *Journal of the American Ceramic Society*. 2019;102(8):4848–4861. <https://doi.org/10.1111/jace.16271>
 32. Potanin A.Yu., Astapov A.N., Pogozhev Yu.S., Rupasov S.I., Shvyndina N.V., Klechkovskaya V.V., Levashov E.A., Timofeev I.A., Timofeev A.N. Oxidation of HfB₂-SiC ceramics under static and dynamic conditions. *Journal of the European Ceramic Society*. 2021;41(16):34–47. <https://doi.org/10.1016/j.jeurceramsoc.2021.09.018>
 33. Hu C., Sakka Y., Tanaka H., Nishimura T., Guo S., Grasso S. Microstructure and properties of ZrB₂-SiC composites prepared by spark plasma sintering using TaSi₂ as sintering additive. *Journal of the European Ceramic Society*. 2010;30(12):2625–2631. <https://doi.org/10.1016/j.jeurceramsoc.2010.05.013>
 34. Hu C., Sakka Y., Gao J., Tanaka H., Grasso S. Microstructure characterization of ZrB₂-SiC composite fabricated by spark plasma sintering with TaSi₂ additive. *Journal of the European Ceramic Society*. 2012;32(7):1441–1446. <https://doi.org/10.1016/j.jeurceramsoc.2011.08.024>
 35. Monteverde F. Ultra-high temperature HfB₂-SiC ceramics consolidated by hot-pressing and spark plasma sintering. *Journal of Alloys and Compounds*. 2007;428(1-2):197–205. <https://doi.org/10.1016/j.jallcom.2006.01.107>
 36. Talmy I.G., Zaykoski J.A., Opeka M.M. High-temperature chemistry and oxidation of ZrB₂ ceramics containing SiC, Si₃N₄, Ta₅Si₃, and TaSi₂. *Journal of the American Ceramic Society*. 2008;91(7):2250–2257. <https://doi.org/10.1111/j.1551-2916.2008.02420.x>
 37. Silvestroni L., Kleebe H.-J. Critical oxidation behavior of Ta-containing ZrB₂ composites in the 1500–1650 °C temperature range. *Journal of the European Ceramic Society*. 2017;37(5):1899–1908. <https://doi.org/10.1016/j.jeurceramsoc.2017.01.020>
 38. Wang S., Xu C., Ding Y., Zhang X. Thermal shock behavior of ZrB₂-SiC composite ceramics with added TaSi₂. *International Journal of Refractory Metals and Hard Material*. 2013;41:507–516. <https://doi.org/10.1016/j.jrmhm.2013.06.010>
 39. Opila E.J., Smith J., Levine S.R., Lorincz J., Reigel M. Oxidation of TaSi₂-containing ZrB₂-SiC ultra-high temperature materials. *The Open Aerospace Engineering Journal*. 2010;3:41–51. <https://doi.org/10.2174/1874146001003010041>
 40. Julian-Jankowiak A., Mathivet V., Justin J.-F., Guérineau V. Development of ultra-high temperature ceramics: from monoliths to composites. *Materials Science Forum*. 2018;941:2041–2046. <https://doi.org/10.4028/www.scientific.net/MSF.941.2041>
 41. Golla B.R., Thimmappa S.K. Comparative study on microstructure and oxidation behaviour of ZrB₂-20vol.% SiC ceramics reinforced with Si₃N₄/Ta additives. *Journal of Alloys and Compounds*. 2019;797:92–100. <https://doi.org/10.1016/j.jallcom.2019.05.097>
 42. Dorner A.N., Werbach K., Hilmas G.E., Fahrenholtz W.G. Effect of tantalum solid solution additions on the mechanical behavior of ZrB₂. *Journal of the European Ceramic Society*. 2021;41(6):3219–3226. <https://doi.org/10.1016/j.jeurceramsoc.2020.12.049>
 43. McClane D.L., Fahrenholtz W.G., Hilmas G.E. Thermal properties of (Zr, TM)B₂ solid solutions with TM = Ta, Mo, Re, V, and Cr. *Journal of the American Ceramic Society*. 2015;98(2):637–644. <https://doi.org/10.1111/jace.13341>
 44. Thimmappa S.K., Golla B.R. Effect of tantalum addition on microstructure and oxidation of spark plasma sintered ZrB₂-20 vol % SiC composites. *Ceramics International*. 2019;45(11):13799–13808. <https://doi.org/10.1016/j.ceramint.2019.04.076>
 45. Thimmappa S.K., Golla B.R., Pitchuka S.B., Prasad B. Nanoindentation and high temperature oxidation behavior of ZrB₂-20SiC-(0–10 wt.%) Ta UHTCs. *Ceramics International*. 2021;47(15):22184–22190. <https://doi.org/10.1016/j.ceramint.2021.04.241>
 46. Yang Y., Qian Y., Xu J., Li M. Effects of TaSi₂ addition on room temperature mechanical properties of ZrB₂-20SiC composites. *Ceramics International*. 2018;44(14):16150–16156. <https://doi.org/10.1016/j.ceramint.2018.05.075>
 47. Ren X., Wang L., Feng P., Zhang P., Guo L., Sun X., Mo H., Li Z. Low temperature synthesis of pure phase TaB₂ powders and its oxidation protection modification behaviors for Si-based ceramic coating in dynamic oxidation environments. *Ceramics International*. 2018;44(13):15517–15525. <https://doi.org/10.1016/j.ceramint.2018.05.212>
 48. Ren X., Wang W., Chen P., Chu H., Feng P., Guo L., Li Z. Investigations of TaB₂ on oxidation-inhibition property and mechanism of Si-based coatings in aerobic environment with broad temperature region for carbon materials. *Journal of the European Ceramic Society*. 2019;39(15):4554–4564. <https://doi.org/10.1016/j.jeurceramsoc.2019.07.020>
 49. Yuan J., Song W., Zhang H., Zhou X., Dong S., Jiang J., Deng L., Cao X. TaZr_{2.75}O₈ ceramics as a potential thermal

- barrier coating material for high-temperature applications. *Materials Letters*. 2019;247:82–85.
<https://doi.org/10.1016/j.matlet.2019.03.102>
50. Liu Q., Hu X., Zhu W., Guo J., Tan Z. Effects of Ta_2O_5 content on mechanical properties and high-temperature performance of $\text{Zr}_6\text{Ta}_2\text{O}_{17}$ thermal barrier coatings. *Journal of the American Ceramic Society*. 2021;104(12):6533–6544. <https://doi.org/10.1111/jace.17990>
51. Yurishcheva A., Astapov A., Lifanov I., Rabinskiy L. High temperature coatings for oxidation and erosion protection of heat-resistant carbonaceous materials in high-speed flows. *Key Engineering Materials*. 2018;771:103–117. <https://doi.org/10.4028/www.scientific.net/KEM.771.103>
52. Corral E.L., Loehman R.E. Ultra-high-temperature ceramic coatings for oxidation protection of carbon-carbon composites. *Journal of the American Ceramic Society*. 2008;91(5):1495–1502.
<https://doi.org/10.1111/j.1551-2916.2008.02331.x>
53. Ren X., Li H., Chu Y., Fu Q., Li K. Preparation of oxidation protective ZrB_2 -SiC coating by in-situ reaction method on SiC-coated carbon/carbon composites. *Surface & Coatings Technology*. 2014;247:61–67.
<https://doi.org/10.1016/j.surfcoat.2014.03.017>
54. Ren X., Li H., Chu Y., Fu Q., Li K. Ultra-high-temperature ceramic HfB_2 -SiC coating for oxidation protection of SiC-coated carbon/carbon composites. *International Journal of Applied Ceramic Technology*. 2015;12(3):560–567. <https://doi.org/10.1111/ijac.12241>
55. Jiang Y., Yin S., Li M., Zhang Z., Tang G., Wang N., Ru H. Oxidation and ablation behaviour of multiphase ultra-high-temperature ceramic $\text{Ta}_{0.5}\text{Zr}_{0.5}\text{B}_2$ -Si-SiC protective coating for graphite. *Ceramics International*. 2021;47(8):11358–11371.
<https://doi.org/10.1016/j.ceramint.2020.12.262>
56. Jiang Y., Wang W., Ru H. Oxidation protection of $(\text{ZrTa})\text{B}_2$ -SiC-Si coating for graphite materials. *Surface Engineering*. 2019;35(4):317–324.
<https://doi.org/10.1080/02670844.2018.1472925>
57. Jiang Y., Liu T., Ru H., Wang W., Zhang C., Wang L. Oxidation and ablation protection of multiphase $\text{Hf}_{0.5}\text{Ta}_{0.5}\text{B}_2$ -SiC-Si coating for graphite prepared by dipping-pyrolysis and reactive infiltration of gaseous silicon. *Applied Surface Science*. 2018;459:527–536.
<https://doi.org/10.1016/j.apsusc.2018.08.042>
58. Wang P., Li H., Ren X., Yuan R., Hou X., Zhang Y. HfB_2 -SiC-MoSi₂ oxidation resistance coating fabricated through in-situ synthesis for SiC coated C/C composites. *Journal of Alloys and Compounds*. 2017;722:69–76.
<https://doi.org/10.1016/j.jallcom.2017.06.008>
59. Ren X., Li H., Fu Q., Li K. $\text{TaHf}_{1-x}\text{B}_2$ -SiC multiphase oxidation protective coating for SiC-coated carbon/carbon composites. *Corrosion Science*. 2014;87:479–488.
<https://doi.org/10.1016/j.corsci.2014.07.016>
60. Ren X., Li H., Li K., Fu Q. Oxidation protection of ultra-high temperature ceramic $\text{Zr}_x\text{Ta}_{1-x}\text{B}_2$ -SiC/SiC coating prepared by in-situ reaction method for carbon/carbon composites. *Journal of the European Ceramic Society*. 2015;35(3):897–907.
<https://doi.org/10.1016/j.jeurceramsoc.2014.09.038>
61. Tong K., Zhang M., Su Z., Wu X., Zeng C., Xie X., Fang C., Yang C., Huang Q., Huang D. Ablation behavior of $(\text{Zr,Ta})\text{B}_2$ -SiC coating on carbon/carbon composites at 2300 °C. *Corrosion Science*. 2021;188:109545.
<https://doi.org/10.1016/j.corsci.2021.109545>
62. Zhou C., Qi Y., Cheng Y., Han W. ZrB_2 -SiC- $\text{Ta}_4\text{HfC}_5/\text{Ta}_4\text{HfC}_5$ oxidation-resistant dual-layer coating fabricated by spark plasma sintering for C/C composites. *Journal of Materials Engineering and Performance*. 2019;28:512–518. <https://doi.org/10.1007/s11665-018-3807-7>
63. Zhang M., Ren X., Chu H., Lv J., Li W., Wang W., Yang Q., Feng P. Oxidation inhibition behaviors of the HfB_2 -SiC- TaSi_2 coating for carbon structural materials at 1700 °C. *Corrosion Science*. 2020;177:108982.
<https://doi.org/10.1016/j.corsci.2020.108982>
64. Wang R., Zhu S., Huang H., Wang Z., Liu Y., Ma Z., Qian F. Low-pressure plasma spraying of ZrB_2 -SiC coatings on C/C substrate by adding TaSi_2 . *Surface & Coatings Technology*. 2021;420:127332.
<https://doi.org/10.1016/j.surfcoat.2021.127332>
65. Ren Y., Qian Y., Xu J., Zuo J., Li M. Ultra-high temperature oxidation resistance of ZrB_2 -20SiC coating with TaSi_2 addition on siliconized graphite. *Ceramics International*. 2019;45(12):15366–15374.
<https://doi.org/10.1016/j.ceramint.2019.05.030>
66. Ren Y., Qian Y., Xu J., Jiang Y., Zuo J., Li M. Oxidation and cracking/spallation resistance of ZrB_2 -SiC- TaSi_2 -Si coating on siliconized graphite at 1500 °C in air. *Ceramics International*. 2020;46(5):6254–6261.
<https://doi.org/10.1016/j.ceramint.2019.11.095>
67. Kannan R., Rangaraj L. Properties of Cf/SiC- ZrB_2 - Ta_xC_y composite produced by reactive hot pressing and polymer impregnation pyrolysis (RHP/PIP). *Journal of the European Ceramic Society*. 2019;39(7):2257–2265.
<https://doi.org/10.1016/j.jeurceramsoc.2019.02.025>
68. Li L., Wang Y., Cheng L., Zhang L. Preparation and properties of 2D C/SiC- ZrB_2 -TaC composites. *Ceramics International*. 2011;37(3):891–896.
<https://doi.org/10.1016/j.ceramint.2010.10.033>
69. Uhlmann F., Wilhelmi C., Schmidt-Wimmer S., Beyer S., Badini C., Padovano E. Preparation and characterization of ZrB_2 and TaC containing Cf/SiC composites via polymer-infiltration-pyrolysis process. *Journal of the European Ceramic Society*. 2017;37(5):1955–1960.
<https://doi.org/10.1016/j.jeurceramsoc.2016.12.048>
70. Tang S., Deng J., Wang S., Liu W., Yang K. Ablation behaviors of ultra-high temperature ceramic composites. *Materials Science and Engineering: A*. 2007;465(1-2):1–7.
<https://doi.org/10.1016/j.msea.2007.02.040>
71. Dunstan D.E., Stokes J. Diffusing probe measurements of polystyrene latex particles in polyelectrolyte solutions: deviations from Stokes-Einstein behavior. *Macromolecules*. 2000;33(1):193–198.
<https://doi.org/10.1021/ma9908503>
72. Li M., Xu Q., Wang L. Thermal conductivity of $(\text{Hf}_{1-x}\text{Zr}_x)_6\text{Ta}_2\text{O}_{17}$ ($x = 0, 0.1, 0.3$ and 0.5) ceramics. *Ceramics International*. 2012;38(5):4357–4361.
<https://doi.org/10.1016/j.ceramint.2011.12.080>
73. Jacobson N.S. Corrosion of silicon-based ceramics in combustion environments. *Journal of the American Ceramic Society*. 1993;76(1):3–28.
<https://doi.org/10.1111/j.1151-2916.1993.tb03684.x>

Information about the Authors



Anna A. Didenko – Cand. Sci. (Eng.), Assistant Professor of the Department of Engineering Graphics, Moscow Aviation Institute (National Research University)

ORCID: 0000-0002-2827-8077

E-mail: yurishcheva@yandex.ru

Alexey N. Astapov – Cand. Sci. (Eng.), Assistant Professor of the Department of Advanced Materials and Technologies for Aerospace Application, Moscow Aviation Institute (National Research University)

ORCID: 0000-0001-8943-2333

E-mail: lexxa1985@inbox.ru

Valentina S. Terentieva – Dr. Sci. (Eng.), Full Professor of the Department of Advanced Materials and Technologies for Aerospace Application, Moscow Aviation Institute (National Research University)

ORCID: 0000-0002-0919-8442

E-mail: k903ter@mai.ru

Сведения об авторах

Анна Александровна Диденко – к.т.н., доцент кафедры «Инженерная графика», Московский авиационный институт (национальный исследовательский университет) (МАИ (НИУ))

ORCID: 0000-0002-2827-8077

E-mail: yurishcheva@yandex.ru

Алексей Николаевич Астапов – к.т.н., доцент кафедры «Перспективные материалы и технологии аэрокосмического назначения», МАИ (НИУ)

ORCID: 0000-0001-8943-2333

E-mail: lexxa1985@inbox.ru

Валентина Сергеевна Терентьева – д.т.н., профессор кафедры «Перспективные материалы и технологии аэрокосмического назначения», МАИ (НИУ)

ORCID: 0000-0002-0919-8442

E-mail: k903ter@mai.ru

Contribution of the Authors



A. A. Didenko – formation of the main concept, search and analysis of the literature, writing the text, formulation of the conclusions.

A. N. Astapov – formation of the main concept, goal and objectives of the study, writing the text, formulation and justification of the heat resistance mechanisms.

V. S. Terentieva – correction of the text and conclusions.

Вклад авторов

А. А. Диденко – формирование основной концепции, поиск и анализ литературы, подготовка текста статьи, формулировка выводов.

А. Н. Астапов – формирование основной концепции, постановка цели и задачи исследования, подготовка текста статьи, формулировка и обоснование механизмов жаростойкости.

В. С. Терентьева – корректировка текста, корректировка выводов.

Received 05.12.2022

Revised 17.12.2022

Accepted 23.12.2022

Статья поступила 05.12.2022 г.

Доработана 17.12.2022 г.

Принята к публикации 23.12.2022 г.